

Constraining Super-light Sterile Neutrino Scenario by JUNO and RENO-50

P. Bakhti* and Y. Farzan†

School of physics, Institute for Research in Fundamental Sciences (IPM)

P.O.Box 19395-5531, Tehran, Iran

(Dated: October 18, 2018)

The Super-light Sterile Neutrino Scenario (SSNS) has been proposed in the literature to explain the suppression of the upturn in the low energy solar data. In this scenario, the mass splitting between the new mass eigenstate, ν_0 and the standard ν_1 is of order of $\Delta m_{01}^2 \sim 10^{-5} \text{ eV}^2$. Reactor neutrino experiments with baseline larger than ~ 20 km can help us to probe this scenario. We study the potential of upcoming JUNO and RENO-50 reactor experiments for discovering the superlight sterile neutrino or constraining its mixing parameters. We study the dependence of sensitivity to the SSNS and find that the proposed JUNO setup is very close to the optimal setup for probing the SSNS.

arXiv:1308.2823v2 [hep-ph] 26 Oct 2013

* pouya_bakhti@ipm.ir

† yasaman@theory.ipm.ac.ir

I. INTRODUCTION

Three neutrino mass and mixing scheme has been established as the solution to the lepton flavor violation observed in solar, atmospheric, reactor and long baseline accelerator neutrino data. Within this scheme, the neutrino oscillation depends on two mass splittings (Δm_{21}^2 and Δm_{31}^2), three mixing angles (θ_{12}, θ_{13} and θ_{23}) and a CP-violating Dirac phase, δ_D . Throughout this letter, we will use the standard parametrization in [1] for the three neutrino scheme. All the neutrino parameters entering neutrino oscillation formula have been measured except for the value of δ_D and $\text{sgn}(\Delta m_{31}^2)$. To determine these last two parameters, studies and various plans are underway.

There are however some anomalies that cannot be explained within the present three neutrino scheme. The most famous examples are the $\nu_\mu \rightarrow \nu_e$ and/or $\bar{\nu}_\mu \rightarrow \bar{\nu}_e$ transitions in short baseline LSND and MiniBooNE experiments [2], reactor neutrino deficit [3] and Gallium anomaly [4]. To explain these anomalies, various scenarios have been suggested among which arguably the most popular one is adding one or more sterile neutrino(s) with mass splitting of order of $O(1)$ eV² with the active ones. With ICECUBE atmospheric neutrino data, this solution can be tested [5]. For a comprehensive study of sterile neutrinos and model building issues, see Refs. [6, 7].

Within the standard LMA MSW solution to the solar puzzle, an upturn of the energy spectrum of events at energies below 8 MeV is expected. However, data from SNO, Super-Kamiokande and Borexino experiments does not display such an upturn. In [8, 9], a scenario is proposed to explain the suppression of the upturn. The scenario is based on adding a new sterile neutrino which weakly mixes with the active neutrinos. The new mass eigenstate is called ν_0 and its mass is denoted by m_0 . To explain the suppression of the upturn in the low energy solar data, it is shown that $\Delta m_{01}^2 \sim (0.7 - 2) \cdot 10^{-5}$ eV² and $\sin^2 2\alpha \sim 10^{-3}$ where α determines the ν_s mixing in ν_1 and/or ν_2 . We refer to this scenario as SSNS standing for Superlight Sterile Neutrino Scenario. Notice however that the low energy solar neutrino data still suffers from large uncertainties and the suppression of the upturn is far from being established. Borexino, KamLAND solar [10] and SNO+ [11] will reduce the uncertainty. Ref. [12] demonstrates that the SSNS can be embedded within a concrete model.

Notice that in this scenario, $\Delta m_{01}^2 \sim \Delta m_{21}^2$. As a result, to test this scenario a long baseline setup such as the ones used to determine mass ordering can be employed. Now that a relatively large value for θ_{13} is established by reactor experiments [13], new phases of these experiments are being studied to help determining the mass hierarchy. JUNO (Jiangmen Underground Neutrino Observatory formerly known as Daya BAY II) [14] and Reno-50 [15] experiments are specifically proposed for this purpose but can also be used for other measurements such as precision measurement of θ_{12} or studies of geoneutrinos [14]. The baseline in these experiments are about 50 km, leading to $\Delta m_{01}^2 L / (2E_\nu) \sim 0.4(\Delta m_{01}^2 / 10^{-5} \text{eV}^2)(L/50 \text{ km})(3 \text{ MeV}/E_\nu)$ so this setup is suitable to search for the effects of a sterile neutrino with $\Delta m_{01}^2 \ll 1$ eV². In this letter, we examine the ability of such long baseline reactor experiments in testing this scenario. We then study the dependence of the sensitivity to SSNS on baseline to search for optimal setup to test the SSNS.

In section II, we describe the four neutrino scenario in which we are interested and outline its new parameters. We then summarize the bounds that already exist on the parameters. In section III, we describe the setups and the inputs for numerical analysis. In section IV, we study oscillation pattern for SSNS and present our results. In section V, we summarize our conclusions.

II. FOUR NEUTRINO SCHEME

The four neutrino mixing matrix can be described by six mixing angles and three physical Dirac phases. If the neutrinos are of Majorana type, there will also be three Majorana CP-violating phases which do not show up in the neutrino oscillation patterns. Following the notation in [9], we call the mass eigenstates as $(\nu_0, \nu_1, \nu_2, \nu_3)$ with mass eigenvalues (m_0, m_1, m_2, m_3) . The flavor eigenstates are related to mass eigenstates by a 4×4 unitary matrix, U as follows

$$\begin{pmatrix} \nu_s \\ \nu_e \\ \nu_\mu \\ \nu_\tau \end{pmatrix} = U \cdot \begin{pmatrix} \nu_0 \\ \nu_1 \\ \nu_2 \\ \nu_3 \end{pmatrix} \quad (1)$$

Notice that ν_0 is not necessarily the lightest state. In fact, Ref. [9] has shown that suppression of the upturn in low energy solar neutrino data implies $m_1 < m_0 < m_2$.

There is a standard way of parameterizing the 3×3 PMNS matrix [1] but there is not such a standard form for the parametrization of the 4×4 mixing matrix. To be compatible with the notation in [9], we use the following parametrization:

$$U \equiv \begin{pmatrix} 1 & 0 \\ 0 & U_{PMNS} \end{pmatrix} \cdot U_S \quad (2)$$

where U_{PMNS} is the standard 3×3 PMNS matrix and U_S is the matrix mixing the sterile neutrino with active ones:

$$U_S = \begin{pmatrix} \cos \alpha & \sin \alpha e^{i\delta_1} & 0 & 0 \\ -\sin \alpha e^{-i\delta_1} & \cos \alpha & 0 & 0 \\ 0 & 0 & 1 & 0 \\ 0 & 0 & 0 & 1 \end{pmatrix} \cdot \begin{pmatrix} \cos \gamma & 0 & \sin \gamma & 0 \\ 0 & 1 & 0 & 0 \\ -\sin \gamma & 0 & \cos \gamma & 0 \\ 0 & 0 & 0 & 1 \end{pmatrix} \cdot \begin{pmatrix} \cos \beta & 0 & 0 & \sin \beta e^{i\delta_2} \\ 0 & 1 & 0 & 0 \\ 0 & 0 & 1 & 0 \\ -\sin \beta e^{-i\delta_2} & 0 & 0 & \cos \beta \end{pmatrix}. \quad (3)$$

To avoid the current bounds we take the mixing between ν_s and active neutrinos to be small. Notice that α and β can be identified with the same parameters in [9]. In the parameter range of our interest where $\Delta m_{01}^2, \Delta m_{20}^2, \Delta m_{21}^2 \ll |\Delta m_{31}^2|$, for intermediate baselines for which $\Delta m_{31}^2 L/E \sim \pi$ (and therefore $\Delta m_{01}^2 L/E \ll \pi$), α and γ parameters cannot be resolved. However, such experiments are sensitive to β . The atmospheric data [16] and long baseline experiment MINOS [17] already constrain

$$\sin^2 \beta < 0.2. \quad (4)$$

A stronger bound comes from cosmology. Recent PLANCK data constrains the effective number of relativistic degrees of freedom at the recombination era, N_{eff} [18]. If β or γ are large enough, ν_s can reach thermal equilibrium at the early universe and can be considered as an extra degree of freedom, contributing $\Delta N_{eff} = 1$. From this observation, Ref. [19] finds $\sin^2 \beta, \sin^2 \gamma < 10^{-3}$ (see also, [16, 20]). One should however remember that there is a deviation between the values of Hubble constant derived from the PLANCK data and from the local measurements. This discrepancy can be settled by an extra degree of freedom [21] so the bounds found in Ref. [19] can be relaxed.

III. JUNO AND RENO-50 EXPERIMENTS

The potential of reactor neutrino experiments with a baseline of ~ 50 km for determining the neutrino mass ordering has been extensively studied in the literature [22–26]. The main goal of JUNO and RENO-50 experiments, which according to schedules [15] will be ready for data taking in 2020, is determining the sign of Δm_{31}^2 . For this purpose as we explain in the next section, high energy resolution is required. Both detectors employ liquid scintillator and aim at an energy resolution of $3\%/\sqrt{E_\nu/\text{MeV}}$. It is shown that in order to determine $\text{sgn}(\Delta m_{31}^2)$, the difference between the distances of different reactors contributing to the flux of the detector should be less than 500 meters [26]. Considering this restriction, the best location for JUNO is found to be at a 52 km distance from Xangjiang and Taishan reactor complexes [26]. The Daya Bay reactor, which is the main contributor to the flux of the current Daya Bay I experiment, is located at a distance of 215 km and the planned Huizhou reactor will be 265 km away. The combined power of the two close reactor complexes is 36 GW. The flux from the far reactors is a troublesome background for the purpose of determining the hierarchy; however, as we shall discuss in the next section for probing the SSNS, the flux from the far sources will also be helpful. The JUNO setup will not have a near detector so the flux normalization uncertainty will be around 3%. As we shall discuss in the next section this uncertainty will not be a problem for probing the SSNS. For our analysis, we use the baselines and powers listed in table 1 of [26] for JUNO.

The RENO-50 setup uses the same reactor used for the current RENO experiment. The baseline for RENO-50 will be 47 km. The total power is 16.4 GW. The near detector can be used to measure the total flux so the flux normalization uncertainty can be reduced to 0.3% [27]. In principle, the KamLAND data could be also used for testing the SSNS. While the total ν flux at KamLAND is comparable to that in JUNO or RENO-50, the new detectors are larger by one order of magnitude. We therefore focus on the JUNO and RENO-50 experiments and do not consider the KamLAND results.

We use the GLoBES software [28] implementing four neutrino scheme [29] for our analysis. We take 20 kton (18 kton) scintillator detector for JUNO (RENO-50) experiment. We assume energy resolution equal to $3\%/\sqrt{E(\text{MeV})}$, and 62 bins are considered from 1.8 MeV to 8 MeV. We employ the energy spectrum for the reactor neutrino as shown in [30, 31]. The cross section of neutrinos is taken from [32]. We take the uncertainties as well as the best fit values of the parameters of the three-neutrino scheme from [33]. We use the pull-method to account for the uncertainties in the parameters of the three neutrino mass scheme. We take the ordering of the mass eigenstates to be normal and set $\delta_D = 0$. According to [14], the main sources of background are (i) accidental background; (ii) $^{13}\text{C}(\alpha, n)^{16}\text{O}$ background and (iii) Geoneutrino background. We take the spectrum of these sources of background from [34] and normalize each background flux as described in [14].

IV. OSCILLATION OF NEUTRINOS

The energy of the reactor neutrinos is of order of a few MeV. At such energies matter effects on the oscillation probability are negligible: $V_{eff} \sim G_F n_e \sim G_F n_n \ll \Delta m_{01}^2/E_\nu < \Delta m_{21}^2/E_\nu \ll |\Delta m_{31}^2/E_\nu|$. The oscillation probability

can be written as

$$P(\bar{\nu}_e \rightarrow \bar{\nu}_e) = |M_0 e^{i\Delta_0} + M_1 e^{i\Delta_1} + M_2 e^{i\Delta_2} + M_3 e^{i\Delta_3}|^2 \quad (5)$$

where $\Delta_i = m_i^2 L / 2E_\nu$ and

$$\begin{aligned} M_0 &= |\cos \beta (-e^{-i\delta_1} \cos \gamma \cos \theta_{12} \cos \theta_{13} \sin \alpha - \cos \theta_{13} \sin \gamma \sin \theta_{12}) - e^{-i(\delta_D + \delta_2)} \sin \beta \sin \theta_{13}|^2, \\ M_1 &= |\cos \alpha \cos \theta_{12} \cos \theta_{13}|^2 \\ M_2 &= |-e^{-i\delta_1} \cos \theta_{12} \cos \theta_{13} \sin \alpha \sin \gamma + \cos \gamma \cos \theta_{13} \sin \theta_{12}|^2 \\ M_3 &= |\sin \beta (-e^{-i\delta_1} \cos \gamma \cos \theta_{12} \cos \theta_{13} \sin \alpha - \cos \theta_{13} \sin \gamma \sin \theta_{12}) + e^{-i(\delta_D + \delta_2)} \cos \beta \sin \theta_{13}|^2. \end{aligned} \quad (6)$$

In the absence of mixing with the sterile neutrinos, we recover the standard formula:

$$P(\bar{\nu}_e \rightarrow \bar{\nu}_e) = |\cos^2 \theta_{13} \cos^2 \theta_{12} e^{i\Delta_1} + \cos^2 \theta_{13} \sin^2 \theta_{12} e^{i\Delta_2} + \sin^2 \theta_{13} e^{i\Delta_3}|^2 \quad (7)$$

The interference of the second and third terms in the oscillation formula (given by $\cos(\Delta_3 - \Delta_2)$) is sensitive to $\text{sgn}(\Delta m_{31}^2)$. To determine the hierarchy, the oscillatory mode given by Δm_{32}^2 has to be resolved which requires excellent energy resolution [35]. Moreover, to resolve this mode, the difference between the distances of different sources should be smaller than the oscillation length associated with Δm_{31}^2 ; otherwise, averaging effects will wash out the sensitivity to the sign. In Eq. (7), there are four oscillatory modes (proportional to $\cos(\Delta_1 - \Delta_2)$, $\cos(\Delta_1 - \Delta_3)$, $\cos(\Delta_3 - \Delta_2)$ and constant) which are in principle enough to determine all the parameters entering Eq. (7), even without the knowledge of the total normalization of the flux. Notice that the CP-violating phase δ_D and mixing angle θ_{23} do not enter Eq. (7) so unlike the case of long baseline experiments, here the derivation of $\text{sign}(\Delta m_{31}^2)$ will not suffer from ambiguity induced by the octant or δ_D degeneracy. The matter effects will cause a deviation of effective mixing angles and mass splittings from the vacuum values of order of 1 %. For the purpose of the precision measurement of θ_{12} and Δm_{21}^2 , matter effects have to be taken into account but for our analysis, we can safely neglect the matter effects.

Let us now discuss the effects of each mixing by the sterile neutrino one by one. In the end, we will discuss the case when all mixings are nonzero.

1. *Case I*, $\sin \beta = \sin \gamma = 0$ and $\alpha \neq 0$: In this limit, the oscillation probability can be written as

$$P(\bar{\nu}_e \rightarrow \bar{\nu}_e) = |\cos^2 \theta_{13} \cos^2 \theta_{12} \sin^2 \alpha e^{i\Delta_0} + \cos^2 \alpha \cos^2 \theta_{13} \cos^2 \theta_{12} e^{i\Delta_1} + \cos^2 \theta_{13} \sin^2 \theta_{12} e^{i\Delta_2} + \sin^2 \theta_{13} e^{i\Delta_3}|^2 \quad (8)$$

By measuring the frequency and amplitude of the oscillatory modes $\cos(\Delta_0 - \Delta_1)$ and/or $\cos(\Delta_0 - \Delta_2)$, the values of α and Δm_{01}^2 can be determined. Notice that to derive these parameters a moderate precision in knowledge of the flux normalization as well as the energy reconstruction resolution will be enough. In other words, the results will not be sensitive to uncertainty in flux normalization or energy resolution. Since $\text{sgn}(\Delta m_{31}^2)$ and $(\alpha, \Delta m_{01}^2)$ are determined by completely separate oscillatory modes, the presence of the mixing α does not affect the determination of $\text{sgn}(\Delta m_{31}^2)$. As expected in the $\Delta m_{01}^2 \rightarrow 0$ limit, the sensitivity to α is lost.

Fig. 1 shows the bound that JUNO and RENO-50 experiments with 5 years of data taking can impose on α . To draw this figure, we have set $\alpha = \beta = \gamma = 0$ and have varied the true value of Δm_{01}^2 using the GLOBES software [28]. For given Δm_{01}^2 the value of $\sin^2 \alpha$ shown by curves can be distinguished from $\alpha = 0$ at 95 % C.L. The blue (thin), red (intermediate) and cyan (thick) curves correspond respectively to the RENO-50, JUNO and combined JUNO and RENO-50 results after 5 years of data taking. As expected for $\Delta m_{01}^2 < 2 \times 10^{-5} \text{ eV}^2$, the bound on $\sin^2 \alpha$ becomes weaker. We also draw plots (not shown here) displaying the minimum $\sin^2 \alpha$ that can be distinguished from $\sin^2 \alpha = 0$. That is we varied the ‘‘true’’ values of Δm_{01}^2 and α , plotting the value of $\sin^2 \alpha$ versus Δm_{01}^2 for which $\sin^2 \alpha = 0$ can be distinguished from it by 95 % C.L. As expected the results were only slightly different from those shown in Fig. 1.

Fig. 1 shows that as $\Delta m_{01}^2 \rightarrow \Delta m_{21}^2$, the sensitivity to $\sin^2 \alpha$ becomes weaker. Moreover at this point, the three curves converge. From Eq (8), it is straightforward to verify that as $\Delta_0 \rightarrow \Delta_2$, the effect of α can be mimicked by a small shift in θ_{12} . Thus, in this limit the bound on $\sin^2 \alpha$ is determined by the uncertainty in θ_{12} : $\sin^2 \alpha < \delta \sin^2 \theta_{12} / \cos^2 \theta_{12}$. Since the effects of θ_{13} are already subdominant the uncertainty in θ_{13} does not affect the sensitivity to α and other new mixing parameters. We have checked this statement by turning off the uncertainty of θ_{13} and θ_{12} one by one. While the uncertainty in θ_{13} seems to be irrelevant, setting the uncertainty in θ_{12} equal to zero, we lose the feature at $\Delta m_{01}^2 \rightarrow \Delta m_{21}^2$. The uncertainty of the solar mass splitting (*i.e.*, $\delta(\Delta m_{21}^2)$) renders the experiment unable to constrain α for $\Delta m_{01}^2 < \delta(\Delta m_{21}^2) \sim 2 \times 10^{-6} \text{ eV}^2$.

Fig. 2 shows the bound that can be derived on $\sin^2 \alpha$ versus baseline for a reactor with 36 GW power and 20 kton detector. For any other values of power and the detector size, the dependence on baseline should be

similar but the curves can be shifted up or down. It is noteworthy that there is a local minimum close to 50 km (close to the baseline of JUNO as well as that of RENO-50) which makes these setups close to ideal for the purpose of probing the SSNS. For $\Delta m_{01}^2 \leq 10^{-5} \text{ eV}^2$, the performance of a setup with baseline farther than 200 km is better. Thus, the Daya Bay or Huizhou reactors or other farther reactor sources contributing to the flux at JUNO can be even more helpful than the closer sources for probing the SSNS. Considering Eq. (8), this is understandable because to discern $\sin^2 \alpha$, $\Delta m_{01}^2 L/E$ should be sizeable.

2. *Case II*, $\sin \alpha = \sin \beta = 0$ and $\gamma \neq 0$: In this limit,

$$P(\bar{\nu}_e \rightarrow \bar{\nu}_e) = \left| \cos^2 \theta_{13} \sin^2 \theta_{12} \sin^2 \gamma e^{i\Delta_0} + \cos^2 \theta_{13} \cos^2 \theta_{12} e^{i\Delta_1} + \cos^2 \theta_{13} \sin^2 \theta_{12} \cos^2 \gamma e^{i\Delta_2} + \sin^2 \theta_{13} e^{i\Delta_3} \right|^2. \quad (9)$$

A discussion similar to case I holds here, too. The only difference is that for $\Delta m_{01}^2 \rightarrow 0$, the sensitivity to γ is limited by $\delta \sin^2 \theta_{12} / \sin^2 \theta_{12}$ but the sensitivity is lost when $\Delta m_{01}^2 \rightarrow \Delta m_{21}^2$ regardless of the uncertainty in $\sin^2 \theta_{12}$. Fig. 3 displays the bound that JUNO and RENO-50 experiments with 5 years of data taking can impose on γ . As expected at $\Delta m_{01}^2 = \Delta m_{21}^2$, the sensitivity to $\sin \gamma$ is lost. The bound on $\sin^2 \alpha$ for $\Delta m_{01}^2 \rightarrow \Delta m_{21}^2$ is about $\tan^2 \theta_{12}$ times the bound on $\sin^2 \gamma$ for $\Delta m_{01}^2 \ll \Delta m_{21}^2$.

Fig. 4 displays the bound that can be imposed on $\sin^2 \gamma$ versus baseline for different values of Δm_{01}^2 favored by the solar data [8, 9]. Independently of Δm_{01}^2 , the optimal baseline is located close to 50 km which means the JUNO and RENO-50 setups, despite being designed for another purpose, are close to optimal setup for probing SSNS, too. Unlike the case I, here there is no other minimum for smaller Δm_{01}^2 . That is because to discern $\sin^2 \gamma$, $\Delta m_{01}^2 L/E$ need not to be sizeable.

3. *Case III*, $\sin \alpha = \sin \gamma = 0$ and $\beta \neq 0$: In this limit,

$$P(\bar{\nu}_e \rightarrow \bar{\nu}_e) = \left| \sin^2 \theta_{13} \sin^2 \beta e^{i\Delta_0} + \cos^2 \theta_{13} \cos^2 \theta_{12} e^{i\Delta_1} + \cos^2 \theta_{13} \sin^2 \theta_{12} e^{i\Delta_2} + \sin^2 \theta_{13} \cos^2 \beta e^{i\Delta_3} \right|^2 \quad (10)$$

By deriving the amplitudes of the oscillatory modes given by $\cos(\Delta_0 - \Delta_1)$ and $\cos(\Delta_0 - \Delta_2)$, the value of $\sin \beta$ can be extracted while the frequency of these modes gives Δm_{01}^2 . Like the case II, sensitivity to $\sin \beta$ persists even in the limit $\Delta m_{01}^2 \rightarrow 0$ so setups with longer baselines have no advantage. Increasing the baseline, the sensitivity to the SSNS deteriorates because of the flux decrease. Similarly to the cases I and II, to derive $\sin \beta$ from these modes a moderate precision in the flux normalization and a moderate energy resolution to reconstruct the modes given by Δm_{01}^2 are sufficient. The amplitudes of the oscillatory $\cos(\Delta_3 - \Delta_1)$ and $\cos(\Delta_3 - \Delta_2)$ terms here are suppressed by $\cos^2 \beta$. For $\beta \ll 1$, this suppression is negligible and $\text{sgn}(\Delta m_{31}^2)$ can be derived, like in the standard case. From Eq. (10), we observe that the sensitivity to $\sin^2 \beta$ is suppressed by a factor of $\sin^2 \theta_{13}$. Thus, as shown in Fig. 5 the bound that can be imposed on $\sin^2 \beta$ by this method is relatively weak; however, they are slightly stronger than the present MINOS bound [17] shown in Eq. (4).

We have found that with 20 years of data taking with JUNO and RENO-50 at $\Delta m_{01}^2 = 2 \times 10^{-5} \text{ eV}^2$, the bound on $\sin^2 \alpha$ and $\sin^2 \gamma$ can be at best lowered down to 2.8×10^{-3} and 4.2×10^{-3} , respectively. For smaller values of Δm_{01}^2 , the bound on $\sin^2 \alpha$ will be weaker but the bound on $\sin^2 \gamma$ will remain the same. Thus, with this setup it is possible to only marginally touch the parameter range indicated in [8, 9] (*i.e.*, $\Delta m_{01}^2 = (0.7 - 2) \times 10^{-5} \text{ eV}^2$ and $\sin^2 \alpha, \sin^2 \gamma \sim 10^{-3}$). By increasing the baseline, Δm_{01}^2 can be resolved better. If the future solar data finds more evidence in support of the SSNS, a setup with multiple sources such as KamLAND but with ~ 20 kton size detector will be a more suitable setup to test SSNS as, unlike the case of determining $\text{sgn}(\Delta m_{31}^2)$, the contributions from different sources add up to determine α and γ .

The following comments are in order:

- As seen from Figures 1, 3 and 5 the performance of JUNO is overallly better than RENO-50. The main reason is that the power of JUNO is considerably larger than that of RENO-50. Moreover as seen in Figs. 2 and 4, the main baseline of JUNO is close to the optimal baseline.
- The background in detectors [14] is low enough not to affect probing the SSNS. We checked for the effects of the background by turning it off and found that the change in results was negligible.
- The interference of the first and third terms in Eqs. (8,9,10) as well as in Eq. (5), which is given by

$$\cos(\Delta_2 - \Delta_0) = \cos(\Delta_2 - \Delta_1) \cos(\Delta_1 - \Delta_0) - \sin(\Delta_2 - \Delta_1) \sin(\Delta_1 - \Delta_0),$$

is already sensitive to the sign of Δm_{01}^2 even though matter effects are suppressed.

- Since the information on new mixing angles come from the oscillating modes with a oscillation length much larger than 1 km, unlike the case of deriving the sign(Δm_{31}^2), here the distance difference between the different sources contributing to the flux is not a cause of concern.
- In the above cases, none of the CP-violating phases appear in $P(\bar{\nu}_e \rightarrow \bar{\nu}_e)$. However, when two or more mixing angles are nonzero, the Dirac CP-violating phases show up in $P(\bar{\nu}_e \rightarrow \bar{\nu}_e)$.
- The dependence of $P(\bar{\nu}_e \rightarrow \bar{\nu}_e)$ on δ_2 and δ_D is through their sum. $P(\bar{\nu}_e \rightarrow \bar{\nu}_e)$ in Eq. (5) enjoys having seven oscillatory modes proportional to $1, \cos(\Delta_0 - \Delta_1), \cos(\Delta_0 - \Delta_2), \cos(\Delta_0 - \Delta_3), \cos(\Delta_1 - \Delta_2), \cos(\Delta_1 - \Delta_3)$ and $\cos(\Delta_2 - \Delta_3)$. In principle, if the amplitudes of all these modes are measured, all mixing angles and the two phases entering Eq. (5) can be extracted. More precisely, by studying the oscillatory modes of the $\bar{\nu}_e$ survival probability, the values of $\theta_{12}, \theta_{13}, \alpha, \beta, \gamma, \delta_1$ and $\delta_2 + \delta_D$ can be extracted. The only degeneracy will be between δ_2 and δ_D which can be broken by a beta-beam or super-beam or neutrino factor facility which measures $P(\nu_e \rightarrow \nu_\mu)$ or $P(\nu_\mu \rightarrow \nu_e)$.
- Drawing these figures, we have taken the ordering of the mass eigenstates to be normal and have set $\delta_D = 0$. As discussed before, in the case that only one of the mixing angles α, β or γ is nonzero, the CP-violating phases do not appear in $P(\bar{\nu}_e \rightarrow \bar{\nu}_e)$ so had we set δ_D equal to some other value, the results would not have changed. The overall behavior does not also depend on the scheme of mass ordering (*i.e.*, normal vs inverted).

V. CONCLUSIONS

We have explored the capacity of the proposed JUNO and RENO-50 setups to probe the SSNS. The mass splitting between the new sterile neutrino ν_0 and the active neutrino ν_1 is taken of order of $\Delta m_{01}^2 \sim 10^{-5} \text{ eV}^2$ and its mixing with ν_1, ν_2 and ν_3 are respectively denoted by α, γ and β . We have studied the bound that can be imposed on these mixing angles if their true values vanish (corresponding to standard three-neutrino mass scheme). We have found that the values of $\sin^2 \alpha$ and $\sin^2 \gamma$ down to a few 10^{-3} can be probed by these setups after five years of data taking. With this setup, it will be possible to marginally probe the parameter space indicated by the low energy solar neutrino data [9]. We have studied the dependence of the sensitivity to baseline and we have found that the JUNO setup is close to an ideal setup for the purpose of probing SSNS. Unlike the case of determining $\text{sgn}(\Delta m_{31}^2)$, farther sources at distances of order of 200-300 km are crucial for improving the sensitivity to SSNS. We have shown that the background and the uncertainty in the flux normalization as well as the energy resolution are not serious issues for improving the sensitivity to the SSNS. As a result, by enlarging the detector size and/or having more numerous and/or powerful sources and/or prolonging the data taking period, the sensitivity to SSNS can be increased to a desired level.

ACKNOWLEDGEMENTS

The authors would like to thank M.M. Sheikh-Jabbari for careful reading of the manuscript. They are also grateful to the anonymous referee for useful remarks. P.B. acknowledges Lashgari for technical help in running the computer codes. Y.F. acknowledges partial support from the European Union FP7 ITN INVISIBLES (Marie Curie Actions, PITN- GA-2011- 289442).

-
- [1] J. Beringer *et al.* [Particle Data Group Collaboration], Phys. Rev. D **86** (2012) 010001.
 - [2] A. Aguilar-Arevalo *et al.* [LSND Collaboration], Phys. Rev. D **64** (2001) 112007 [hep-ex/0104049]; A. A. Aguilar-Arevalo *et al.* [MiniBooNE Collaboration], Phys. Rev. Lett. **110** (2013) 161801 [arXiv:1207.4809 [hep-ex], arXiv:1303.2588 [hep-ex]].
 - [3] T. A. Mueller, D. Lhuillier, M. Fallot, A. Letourneau, S. Cormon, M. Fechner, L. Giot and T. Lasserre *et al.*, Phys. Rev. C **83** (2011) 054615 [arXiv:1101.2663 [hep-ex]].
 - [4] J. N. Abdurashitov, V. N. Gavrin, S. V. Girin, V. V. Gorbachev, P. P. Gurkina, T. V. Ibragimova, A. V. Kalikhov and N. G. Khairnasov *et al.*, Phys. Rev. C **73** (2006) 045805 [nucl-ex/0512041]; J. Kopp, P. A. N. Machado, M. Maltoni and T. Schwetz, JHEP **1305** (2013) 050 [arXiv:1303.3011 [hep-ph]].
 - [5] A. Esmaili and A. Y. Smirnov, arXiv:1307.6824 [hep-ph].
 - [6] K. N. Abazajian, M. A. Acero, S. K. Agarwalla, A. A. Aguilar-Arevalo, C. H. Albright, S. Antusch, C. A. Argüelles and A. B. Balantekin *et al.*, arXiv:1204.5379 [hep-ph].
 - [7] A. Merle, arXiv:1302.2625 [hep-ph].

- [8] P. C. de Holanda and A. Yu. Smirnov, Phys. Rev. D **69** (2004) 113002 [hep-ph/0307266].
- [9] P. C. de Holanda and A. Yu. Smirnov, Phys. Rev. D **83** (2011) 113011 [arXiv:1012.5627 [hep-ph]].
- [10] Y. Kishimoto [KamLAND collaboration], J. Phys. Conf. Ser. **120** (2008) 52010.
- [11] M. C. Chen [SNO+ Collaboration], arXiv:0810.3694 [hep-ex]; C. Kraus and S. J. M. Peeters [SNO+ Collaboration], Prog. Part. Nucl. Phys. **64** (2010) 273.
- [12] P. S. B. Dev and A. Pilaftsis, arXiv:1212.3808 [hep-ph].
- [13] F. P. An *et al.* [DAYA-BAY Collaboration], Phys. Rev. Lett. **108**, 171803 (2012) [arXiv:1203.1669 [hep-ex]]; J. K. Ahn *et al.* [RENO Collaboration], Phys. Rev. Lett. **108**, 191802 (2012) [arXiv:1204.0626 [hep-ex]]; Y. Abe *et al.* [DOUBLE-CHOOZ Collaboration], Phys. Rev. Lett. **108**, 131801 (2012) [arXiv:1112.6353 [hep-ex]].
- [14] S. Kettell, J. Ling, X. Qian, M. Yeh, C. Zhang, C. -J. Lin, K. -B. Luk and R. Johnson *et al.*, arXiv:1307.7419 [hep-ex].
- [15] <http://home.kias.re.kr/MKG/h/reno50>.
- [16] M. Cirelli, G. Marandella, A. Strumia and F. Vissani, Nucl. Phys. B **708** (2005) 215 [hep-ph/0403158].
- [17] P. Adamson *et al.* [MINOS Collaboration], Phys. Rev. D **81** (2010) 052004 [arXiv:1001.0336 [hep-ex]].
- [18] P. A. R. Ade *et al.* [Planck Collaboration], arXiv:1303.5076 [astro-ph.CO].
- [19] A. Mirizzi, G. Mangano, N. Saviano, E. Borriello, C. Giunti, G. Miele and O. Pisanti, arXiv:1303.5368 [astro-ph.CO].
- [20] A. D. Dolgov and F. L. Villante, Nucl. Phys. B **679** (2004) 261 [hep-ph/0308083].
- [21] M. Wyman, D. H. Rudd, R. A. Vanderveld and W. Hu, arXiv:1307.7715 [astro-ph.CO]; M. Archidiacono, E. Giusarma, S. Hannestad and O. Mena, arXiv:1307.0637 [astro-ph.CO].
- [22] A. Bandyopadhyay, S. Choubey, S. Goswami and S. T. Petcov, Phys. Rev. D **72** (2005) 033013 [hep-ph/0410283]; A. Bandyopadhyay, S. Choubey and S. Goswami, Phys. Rev. D **67** (2003) 113011 [hep-ph/0302243]; S. Choubey, S. T. Petcov and M. Piai, Phys. Rev. D **68** (2003) 113006 [hep-ph/0306017]; S. T. Petcov and M. Piai, Phys. Lett. B **533** (2002) 94 [hep-ph/0112074]; J. Learned, S. T. Dye, S. Pakvasa and R. C. Svoboda, Phys. Rev. D **78** (2008) 071302 [hep-ex/0612022]; L. Zhan, Y. Wang, J. Cao and L. Wen, Phys. Rev. D **79** (2009) 073007 [arXiv:0901.2976 [hep-ex]]; L. Zhan, Y. Wang, J. Cao and L. Wen, Phys. Rev. D **78** (2008) 111103 [arXiv:0807.3203 [hep-ex]]; S. -F. Ge, K. Hagiwara, N. Okamura and Y. Takaesu, JHEP **1305** (2013) 131 [arXiv:1210.8141 [hep-ph]].
- [23] M. Blennow and T. Schwetz, arXiv:1306.3988 [hep-ph].
- [24] E. Ciuffoli, J. Evslin and X. Zhang, arXiv:1302.0624 [hep-ph].
- [25] E. Ciuffoli, J. Evslin, Z. Wang, C. Yang, X. Zhang and W. Zhong, arXiv:1308.0591 [hep-ph].
- [26] Y. -F. Li, J. Cao, Y. Wang and L. Zhan, arXiv:1303.6733 [hep-ex].
- [27] S.-H. Seo, talk at International Workshop on “RENO-50” toward Neutrino Mass Hierarchy, 13-14 June 2013, Seoul National University, Korea.
- [28] P. Huber, M. Lindner and W. Winter, Comput. Phys. Commun. **167**, 195 (2005) [hep-ph/0407333]; P. Huber, J. Kopp, M. Lindner, M. Rolinec and W. Winter, Comput. Phys. Commun. **177**, 432 (2007) [hep-ph/0701187]; <http://www.mpi-hd.mpg.de/personalhomes/globes>.
- [29] J. Kopp, M. Lindner, T. Ota and J. Sato, Phys. Rev. D **77** (2008) 013007 [arXiv:0708.0152 [hep-ph]]; J. Kopp, Int. J. Mod. Phys. C **19** (2008) 523 [physics/0610206].
- [30] H. Murayama and A. Pierce, Phys. Rev. D **65** (2002) 013012 [hep-ph/0012075].
- [31] K. Eguchi *et al.* [KamLAND Collaboration], Phys. Rev. Lett. **90** (2003) 021802 [hep-ex/0212021].
- [32] P. Vogel and J. F. Beacom, Phys. Rev. D **60** (1999) 053003 [hep-ph/9903554].
- [33] M. C. Gonzalez-Garcia, M. Maltoni, J. Salvado and T. Schwetz, JHEP **1212** (2012) 123 [arXiv:1209.3023 [hep-ph]].
- [34] A. Gando *et al.* [KamLAND Collaboration], arXiv:1303.4667 [hep-ex].
- [35] F. Capozzi, E. Lisi and A. Marrone, arXiv:1309.1638 [hep-ph].

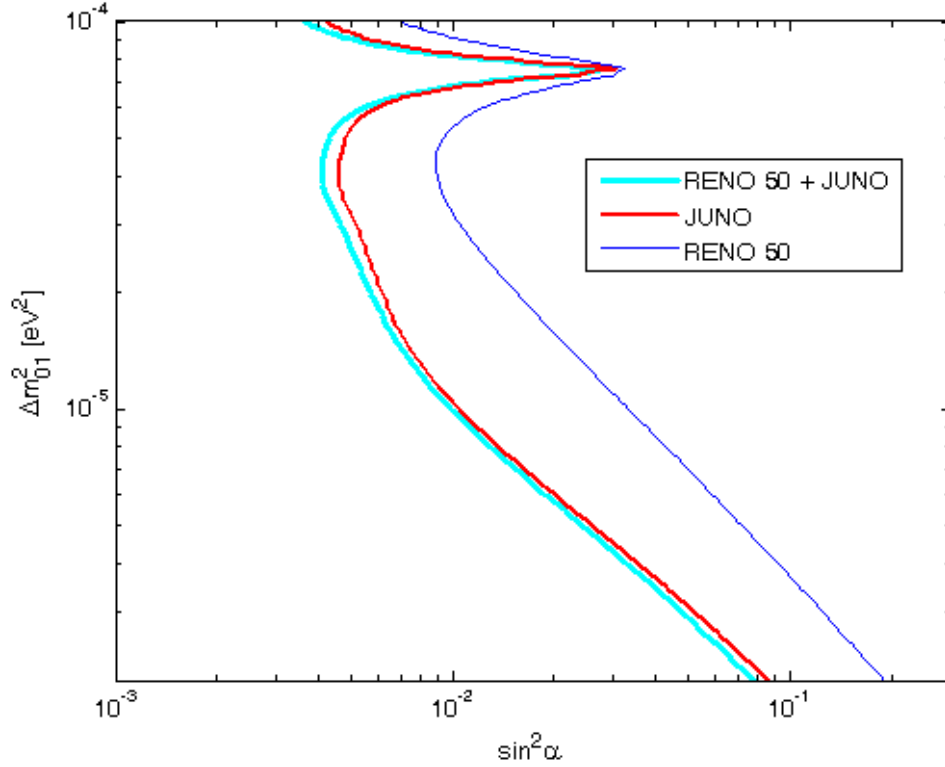


FIG. 1. The 95% C.L. upper bound on $\sin^2 \alpha$ versus Δm_{01}^2 . Five years of data taking with JUNO and RENO-50 experiments are assumed. The true values of α , γ and β are set to zero. The blue (thin), red (intermediate) and cyan (thick) curves correspond respectively to the RENO-50, JUNO and combined JUNO and RENO-50 performances. The values of the parameters of the three neutrino mass scheme are set to the best values found in Ref. [33] and the same uncertainties are assumed. We have taken the ordering of the mass eigenstates to be normal and have set $\delta_D = 0$.

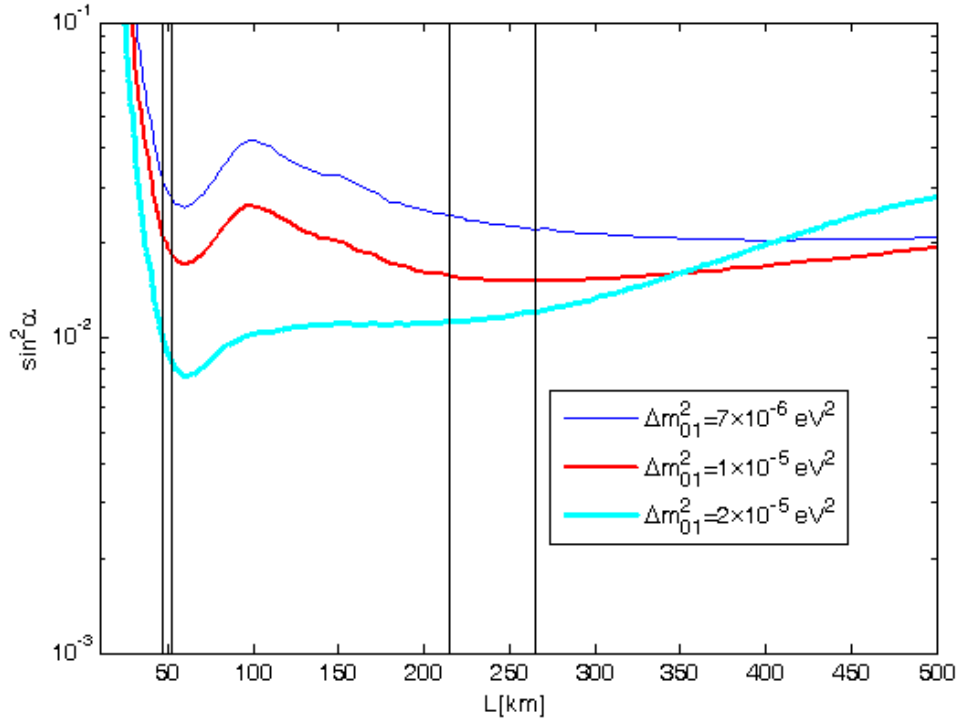


FIG. 2. The 95% C.L. upper bound on $\sin^2 \alpha$ versus the baseline. Five years of data taking with a 20 kton detector and 36 GW reactor source are assumed. The true values of α , γ and β are set to zero. The cyan (thick), red (intermediate) and blue (thin) curves correspond respectively to $2 \times 10^{-5} \text{ eV}^2$, 10^{-5} eV^2 and $0.7 \times 10^{-5} \text{ eV}^2$. The values of the parameters of the three neutrino mass scheme are set to the best values found in Ref. [33] and the same uncertainties are assumed. We have taken the ordering of the mass eigenstates to be normal and have set $\delta_D = 0$. From left to right, the vertical lines show the baseline of RENO-50, the distance between the JUNO detector to the Taishan or Xangjiang reactors, the distance between the JUNO detector to the Daya Bay reactor and the distance between the JUNO detector to the Huizhou reactor.

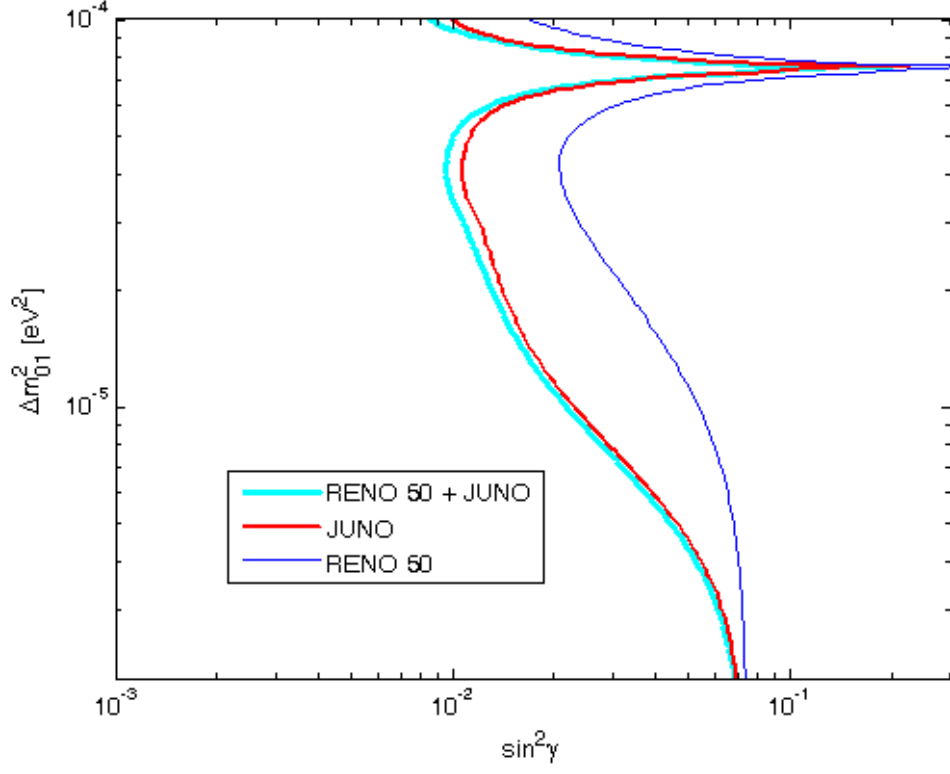


FIG. 3. The 95% C.L. upper bound on $\sin^2 \gamma$ versus Δm_{01}^2 . The rest of the description is similar to that of Fig. 1.

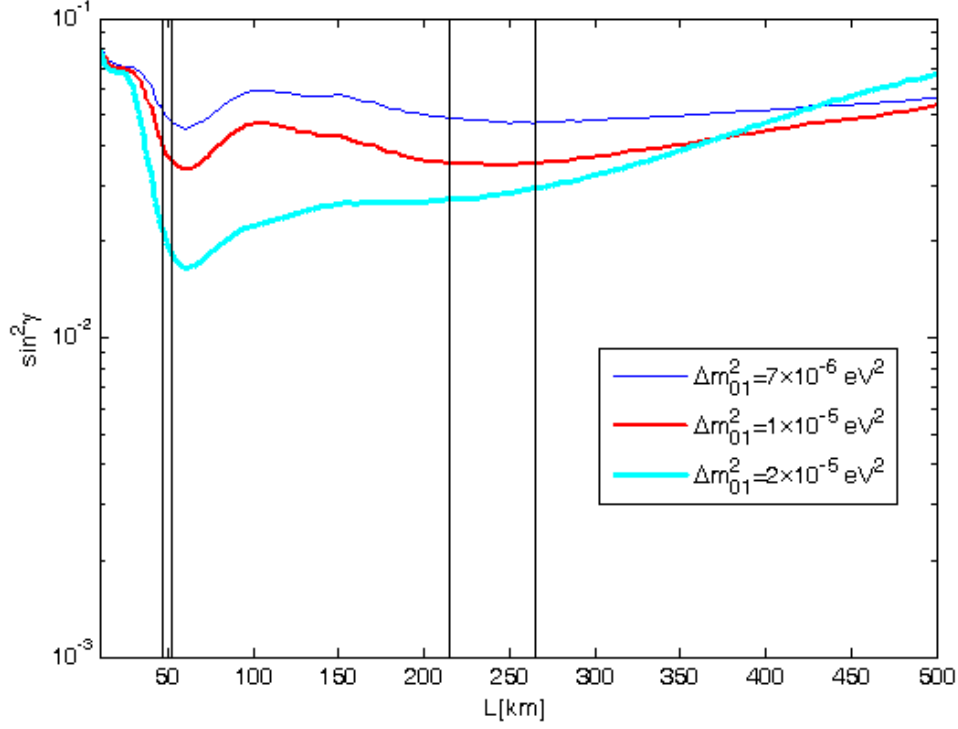


FIG. 4. The 95% C.L. upper bound on $\sin^2 \gamma$ versus the baseline. The rest of the description is similar to that of Fig. 2.

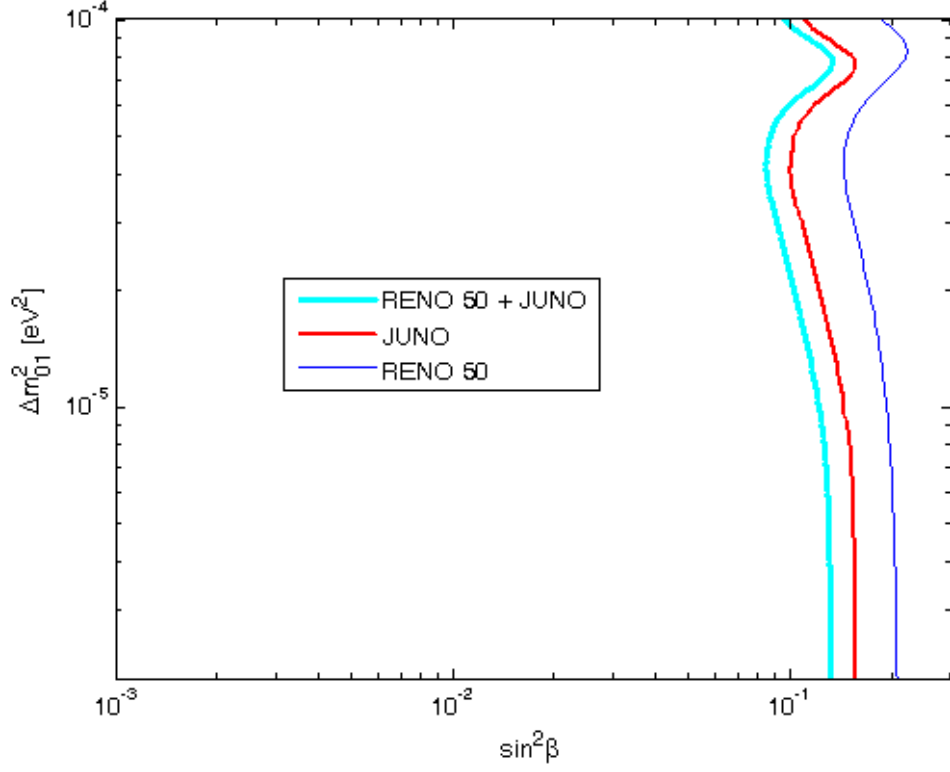


FIG. 5. The 95% C.L. upper bound on $\sin^2 \gamma$ versus Δm_{01}^2 . The rest of the description is similar to that of Fig. 1.